Optical and Quantum Electronics (2023) 55:536
https://doi.org/10.1007/s11082-023-04796-8

Predicting structural, optoelectronic and mechanical properties of germanium based $AGeF_3$ (A = Ga and In) halides perovskites using the DFT computational approach

Mudasser Husain[1] · Nasir Rahman[1] · Mongi Amami[2] · Tahir Zaman[3] · Mohammad Sohail[1] · Rajwali Khan[1] · Abid Ali Khan[4] · Saima Ahmad Shah[5] · Saeedullah[6] · Aurangzeb Khan[7,8] · Ali H. Reshak[9,10,11] · Nora Hamad Al-Shaalan[12] · Sarah Alharthi[13,14] · Saif A. Alharthy[15,16] · Mohammed A. Amin[13] · Vineet Tirth[17,18]

Received: 28 September 2022 / Accepted: 23 March 2023

Abstract
The increasing research of advanced materials with tremendous compositional and structural degrees of variation, identifying and discovering new materials for a specific application is a challenging task. Here, we report for the first time the predicted structural, optoelectronic, and mechanical properties of germanium based $AGeF_3$ (A = Ga and In) halides Perovskites using the density functional theory computational approach. The tolerance factor "τ" is computed for both the materials and is found to be 0.91 for $InGeF_3$ and 0.89 for $GaGeF_3$ which indicates the structural stability of these perovskites crystal structures. The optimized crystal structural parameters for both the compounds are found to be 4.476 Å for $InGeF_3$ and 4.422 Å for $GaGeF_3$ by performing the fit using Birch–Murnaghan for the unit cell energy verses unit cell volume. Using the optimized lattice constants all the basic physical properties are computed. From the results of electronic properties it is determined that both the compounds depict a semiconductor nature with having an indirect (R-M) band gap of 1.48 eV for $InGeF_3$ and 0.98 eV for $GaGeF_3$. To explore the potential of these selected compounds the optical properties within the energy range of 0 eV up to 40 eV incident photon are computed for the prospective optoelectronic applications. Moreover, the mechanical properties for both the materials are computed using the IRelast package and the values of cubic elastic parameters estimates that $AGeF_3$ (A = Ga and In) halides Perovskites are mechanically stable, hard to scratch, ductile and anisotropic. We are fully confident on the precision and accuracy of our reported results and reveals that the applications of germanium based $AGeF_3$ (A = Ga and In) halides Perovskites compounds can be deemed in photovoltaic and in modern semiconducting industries.

Keywords WIEN2K · IRelast package · DFT · Structural properties · Optoelectronic properties · Mechanical properties

✉ Nasir Rahman
nasir@ulm.edu.pk

Extended author information available on the last page of the article

Published online: 14 April 2023

1 Introduction

The calcium titanate ($CaTiO_3$) was regarded as the beginning of perovskite, and minerals with similar crystal structure as calcium titanate are referred to as perovskite materials. For perovskite materials ABX_3 is the standard chemical formula, where "A" and "B" are metallic cations with "A" being larger than "B" and "X" being the anion, which is commonly oxides or halogens group elements. For numerous optoelectronic and photonic device applications (Shuvo et al. 2022), Perovskite compounds have been identified as among the most potential and convenient low-cost energy materials (Körbel et al. 2016; Nishimatsu et al. 2002; Khondoker et al. 2022). Perovskite materials possess an unusual physical features like high absorption coefficient, high dielectric constant (Ahmed et al. 2021), long-range ambipolar charge transfer, ferroelectric properties (Molla et al. 2022) and low exciton-binding energy etc. have sparked a lot of interest in photovoltaic (Labrim xxxx; Erum and Iqbal 2017) and optoelectronic applications (Sohail et al. 2022; Seddik et al. 2012; Mitro et al. 2022a). Various types of perovskite materials were researched extensively, including "AMO_3" (chalcogenides perovskite) also known as organo-metal halide and halide perovskite (ABX_3) (Hossain 2022). Besides that, the perovskite crystal seems to have an area for imprinting some physical properties with numerous applications (Haq et al. 2021), including giant magnetoresistance (Kim et al. 2001) nearly zero temperature coefficient of resistivity (Chi et al. 2001), tunable laser (Manaa et al. 1993), laser source (Bloomstein et al. 1999), electron–phonon interactions (Lucas et al. 1995; Avram et al. 2005), crystal fields (Lahoz et al. 1997), phase transition behavior, and some other physical properties like, anti-ferromagnetism (Vaitheeswaran et al. 2010), ferro-electricity (Berastegui et al. 2001) and semi-conductivity (Daniels et al. 1983). Furthermore, fluoroperovskites compounds can be utilized in the medical field to quantify dose during radiation therapy, and also in the production of radiation imaging plates for gamma-rays, X-rays, and thermal neutrons for medical and non-destructive testing (Donaldson et al. 2014). The mechanical and thermal endurance of fluoroperovskites compounds are characterized by their wide energy band gap and low hygroscopicity. Simulating the behavior of materials has become possible as computational power has increased (Wang et al. 2023; Liu et al. 2022; Wei et al. 2022). This allows materials scientists to better understand behavior and mechanisms, develop novel materials, and explain previously unknown features (Wu et al. 2022; Fan et al. 2020; Li et al. 2022). Integrated computational materials engineering efforts are currently concentrating on merging computational approaches with experiments to substantially minimize the time and effort required to optimize material properties for a specific application (Santello et al. 2019; Zhang et al. 2022; Zhong et al. 2022a). This includes applying methods like density functional theory (Obot et al. 2015; Zheng et al. 2022), molecular dynamics (Hansson et al. 2002; Chen et al. 2022), Monte Carlo (Mooney 1997; Zhong et al. 2022b), dislocation dynamics, phase field, finite element, and others to simulate materials at all length scales. For lead-free and long-term power conversion efficiency of the PSCs (perovskite solar cells), the germanium-based inorganic perovskites $AGeF_3$ (A = Ga and In) compounds have shown promise as substitutes for tin-based perovskites (Jong et al. 2019; Alam et al. 2022; Mitro et al. 2022b). We choose the Germanium based $AGeF_3$ (A = Ga and In) compounds belong to halides Perovskites in which the base element is the germanium for the computation of different physical properties using DFT within the WIEN2K code (Blaha et al. 2001). There is no theoretical and experimental results reported yet for the selected fluoroperovskites and

we intend to investigate computationally for the first the properties of these perovskites which will provide a reference frame for the experimental scientists.

2 Computational research methodologies

In this research work, the investigations of structural, mechanical, and optoelectronic properties is done using the method of first-principle investigations by implying DFT approach within the WIEN2K (Blaha et al. 2001) computational simulation package. The ground state is characterized using the FP-LAPW (full-potential linearized-augmented plane wave) (Blaha et al. 1990) approach which is applied in the WIEN2K program based on density functional theory. It is a fundamental quantum mechanical framework for many-body problems that has proven to be among the most precise approaches for calculating physical properties. The TB-mBJ (Tran–Blaha modified Becke–Johnson) (Camargo-Martínez and Baquero 2012) exchange potential is utilized to explore the electronic, optical and thermoelectric characteristics of the germanium based $AGeF_3$ (A = Ga and In) halides Perovskites compounds. The valence and core electrons are respectively considered as semi and fully relativistic. The compound's unit cell is separated into two domains, the first of which is the interstitial zone. To accomplish energy eigenvalue convergence, the plane wave is created in this zone with a cutoff value of $K_{max} = 8.0/Rmt$. The $K_{max} and Rmt$ are the magnitudes of the largest K-vector and the smallest radius of non-overlapping atomic spheres in the plane wave expansion. The *Rmt* are considered to be 2.50, 1.05 and 1.88 atomic unit (a.u) for A = Ga and In, Ge and F atoms, respectively. The non-overlapping muffin-tin spheres is another domain, where the spherical harmonics wave develops around $l_{max} = 14$, and at $G_{max} = 20\left[Ry\right]^{1/2}$ the Fourier charge density expands. In the "IBZ" (irreducible Brillouin zone) the self-consistency convergence occurred with 56 k-points with a K-mesh of $12 \times 12 \times 12$ grid. The convergence of charge and energy is thought to occur when both are less than $0.19 \times 10^3 e$ and $0.19 \times 10^3\ Ry/atom$. Using these computational approach we intend to investigate some of the physical properties of selected germanium based $AGeF_3$ (A = Ga and In) halides Perovskites compounds by providing a framework data on these materials for the experimental scientist.

3 Results and discussion

The investigated results computed for selected germanium based $AGeF_3$ (A = Ga and In) halides Perovskites compounds using the reported computational approach are deeply discussed in this portion.

3.1 Analysis of structural properties

The objective of the analysis of structural properties of the selected materials is to know its structural stability and its formation. The Goldschmidt's tolerance factor (Bartel et al. 2019) which indicates the stability and distortion of crystal structures is computed for both the compounds by using the expression:

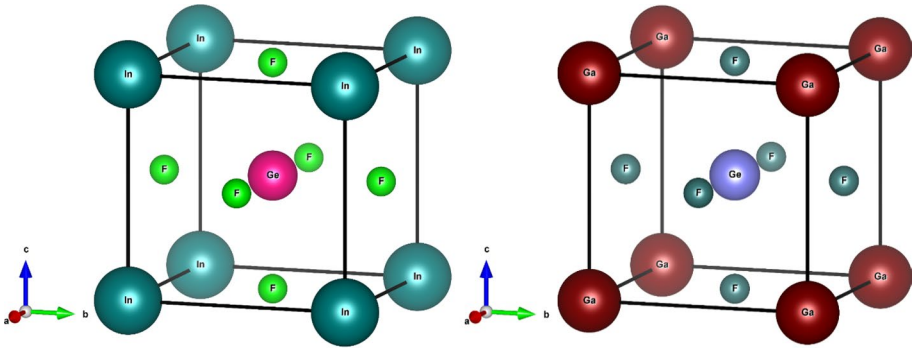

Fig. 1 The $AGeF_3$ (A = Ga and In) halides Perovskites crystalizes in cubic symmetry

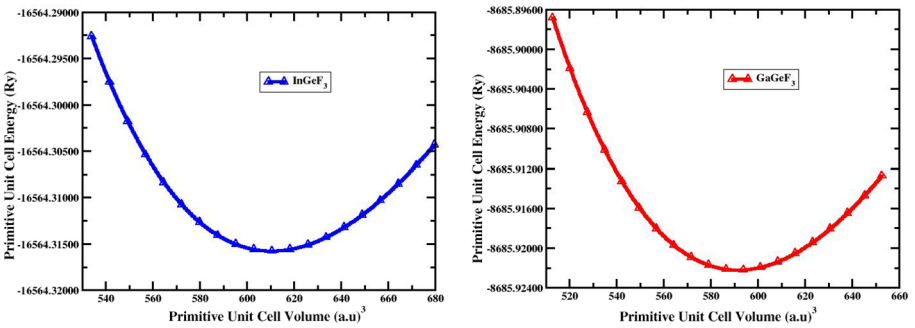

Fig. 2 The optimized curve of $AGeF_3$ (A = Ga and In) halides Perovskites crystalizes in cubic symmetry

$$\tau = \frac{r_A + r_B}{\sqrt{2}\left(r_B + r_X\right)} \tag{1}$$

whereas "r_A" and "r_B" and "r_X" represents the ionic radii of A, B and X atoms respectively.

The measured values of "τ" is found to be 0.91 for $InGeF_3$ and 0.89 for $GaGeF_3$ which indicates the structural stability of these crystal structures. The germanium based $AGeF_3$ (A = Ga and In) halides Perovskites crystalizes in cubic symmetry with atomic positions for "A = Ga and In" is (0, 0, 0), "Ge" at (0.5, 0.5, 0.5) and for "F" is (0, 0.5, 0.5) or (0.5, 0, 0.5) or (0.5, 0.5, 0) as shown in the Fig. 1.

In order to find the structural optimized lattice parameters the Birch Murnaghan fit curve of primitive unit cell energy verses the primitive unit cell volume is achieved. The Fig. 2 depicts the optimized fitted curve which shows that the unit cell energy become optimized when the corresponding unit cell volume increases. A point will reaches where the energy and volume will be fixed.

The investigations of structural properties for the selected materials confirm that both the materials are structurally stable and possess in a cubic crystal structure. The computed optimized structural parameters are shown in Table 1.

Table 1 The illustrations of optimized crystal structural parameters including the lattice constant "a_0", tolerance factor "τ", bulk modulus "B" in GPa, $B^{/}$ (the derivative of bulk modulus) in GPa, ground state energy E_0 in "Ry" and the ground state volume "V_0" in $(a.u)^3$

Structural parameters	$InGeF_3$	$GaGeF_3$
a_0 in Å	4.476	4.422
B	58.94	56.76
$B^{/}$	4.97	5.28
E_0	− 16,564.32	− 8685.92
V_0	613.86	593.77
τ	0.91	0.89

3.2 The analysis of electronic properties

In this section we focus on the analysis of electronic properties of germanium based $AGeF_3$ (A = Ga and In) halides Perovskites by computing the electronic band structures and density of states (DOS). The term "band structure" refers to the electron states in crystalline semiconductors that are described by a quantum mechanical theory. Herein, the intrinsic gap of semiconductors is computed through the TB-mBJ approximation (Dufek et al. 1994; Charifi et al. 2005; El haj Hassan et al. 2004). Following that, the predicted band energies are illustrated for various wave-vector "k" values located along high symmetry lines in the first Brillouin zone. Figure 3 depicts the predicted energy band structures for the selected compounds at the equilibrium geometry along the directions of higher symmetries in the Brillouin zone. In order to allow each state to be identified by the associated value of k in the first Brillouin zone, the regions of permitted energies are separated into bands in ascending order. The Fermi energy level (E_F) is taken at 0 eV energy shown by dotted

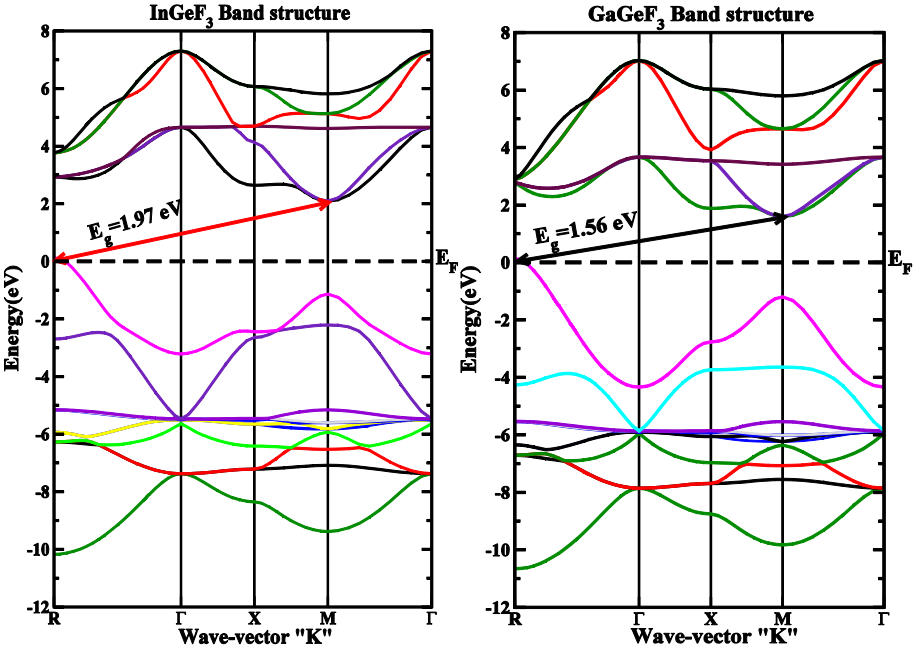

Fig. 3 The investigated band structures of $AGeF_3$ (A = Ga and In) halides Perovskites

horizontal line and the level is coincide with the valence band. The computed electronic bands structure for the compounds of interest are semiconducting with the E_g (energy band gap) of 1.48 eV for $InGeF_3$ and for $GaGeF_3$ the "E_g" is 0.98 eV. Both the materials possess an indirect band gaps from (R-M) symmetry points which predict the applications of the selected materials in semiconducting and optoelectronic devices.

The TDOS and PDOS (total and partial atomic densities of states) for germanium based $AGeF_3$ (A = Ga and In) halides Perovskites are depicted in Fig. 4 to provide a better understanding of the electronic properties. The DOS is plotted at the energy range of − 8–8 eV and the vertically dotted line is the Fermi energy level (E_F) lies at the 0 eV. The portion from − 8 to 0 eV shows the valence band (VB) while from 0 to 8 eV depict the conduction band (CB). It can be clearly seen that the major states contribution in the valence band is from the F-*p* state of an atom, while in the conduction band the contribution to the states occurs from the In-*p*, Ge-*p* states. There exist a band gap which is fully consistent with the electronic bands and this confirm the accuracy of our results. These contributions of different elemental states confirm that the materials possess a semiconducting nature and the application can be deemed in many semiconducting industries.

3.3 The analysis of elastic properties

In this section we describe the investigated results of the elastic properties in detail for germanium based $AGeF_3$ (A = Ga and In) halides Perovskites using the computational computing code of IRelast (Jamal et al. 2018). The elastic constants are crucial in defining the mechanical properties of materials because they control how a crystal reacts to outside forces. The measurements of these constants offer important knowledge about the stiffness and stability of materials. For this reason, the energy as a function of lattice strain with retained volume is used to compute the components of the stress tensor for tiny strains, which allowed for the calculation of the elastic constants of the material of interest at zero pressure. The cubic crystal lattice's symmetry limits the number of distinct elastic constants C_{ij} to three i.e., C_{11}, C_{12} and C_{44} from the total of 21. Table 2 shows the investigated cubic C_{ij} (elastic constants) for $AGeF_3$ (A = Ga and In) halides Perovskites. There is some requirements for the mechanical stability of the cubic crystal which are $C_{11} - C_{12} > 0$, $C_{11} > 0$, $C_{44} > 0$, $C_{11} - 2C_{12} > 0$ (Wang et al. 1993) to be satisfied. Our

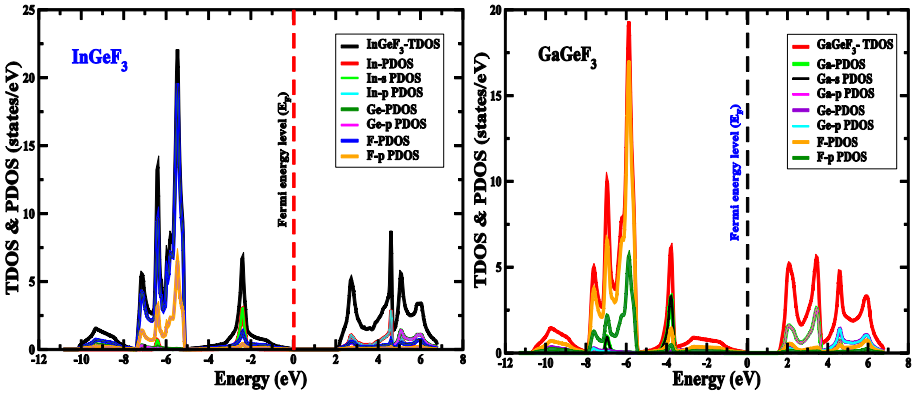

Fig. 4 The investigated TDOS and PDOS of $AGeF_3$ (A = Ga and In) halides Perovskites

Table 2 The computed cubic elastic constants C_{ij} (C_{11}, C_{12} and C_{44}) in GPa, Bulk modulus "B", Young's modulus "E" in GPa, Shear modulus "G" in GPa, anisotropy factor "A", Poisson ratio "υ", the Pugh ratio (B/G), machinability index μ_M, and Vickers hardness "H_v" for germanium based $AGeF_3$ (A = Ga and In) halides Perovskites

Elastic parameters	$InGeF_3$	$GaGeF_3$
C_{11}	88.74	78.35
C_{12}	43.74	36.89
C_{44}	20.51	18.93
E	36.87	37.73
G	13.67	11.96
A	3.43	4.68
υ	0.92	0.78
B	58.94	56.76
B/G	4.31	4.74
μ_M	2.87	2.99
H_v	5.64	3.87

computed results of C_{ij} for the selected germanium based $AGeF_3$ (A = Ga and In) halides Perovskites satisfy the criteria and are considered to be elastically stable. Understanding a material's mechanical properties is important since they have a significant impact on the manufacture, processing, and durability of the device.

If the strain is not too great as to defy Hook's rule, elastic constants C_{11}, C_{12} and C_{44} can be used to measure the relationship between strain and stress in a crystal. When computing the elastic constant, a crystal is subjected to a strain, the energy versus strain is measured, and the elastic constant is calculated from the curvature of this function at zero strain. A specific linear configuration of elastic constants corresponds to a given strain. The ability to cause micro-cracks in materials is strongly correlated with the elastic anisotropy of crystals, which has significant implications for engineering research. The elastic anisotropy "A" of these $AGeF_3$ (A = Ga and In) halides Perovskites compounds is 3.43 for $InGeF_3$ and 4.68 for $GaGeF_3$ and is investigated using the equation:

$$A = \frac{2C_{44}}{(C_{11} - C_{12})} \tag{2}$$

A is equal to "1" for an entirely isotropic material, and any number other than "1" denotes anisotropy. The magnitude of the variation from "1" serves as a gauge for the crystal's level of elastic anisotropy and the values of "A" confirm that both the materials are anisotropic. The elastic moduli and Poisson ratio is the key parameters used to characterize the mechanical stability of a material and is computed using the relations (Hill 1952; Voigt 1928).

$$E = \frac{9GB}{3B + G} \tag{3}$$

$$\upsilon = \frac{3B - 2G}{2(3B + G)} \tag{4}$$

$$G_V = \frac{1}{5}\left(C_{11} - C_{12} + 3C_{44}\right) \tag{5}$$

$$G_R = \frac{5C_{44}\left(C_{11} - C_{12}\right)}{4C_{44} + 3\left(C_{11} - C_{12}\right)} \tag{6}$$

Table 2 shows the computed values of elastic moduli and Poisson ratio for germanium based $AGeF_3$ (A = Ga and In) halides Perovskites. The material's deformation in a direction perpendicular to the direction of the applied force is measured by "υ" (Poisson's ratio). The computed and reported values of "υ" for $InGeF_3$ is 0.92 and that for $GaGeF_3$ is 0.78 which depict that the deformation in these materials in the perpendicular direction of force is very difficult. The Frantsevich rule (Frantsevich 1982) states that the material's critical value of "υ" is 0.26. Poisson's ratio must be smaller than 0.26 for brittle materials; otherwise, the material will act ductile. To talk about a material's ductile or brittle nature depends on a variety of parameters. One of the remarkable parameter for differentiating the ductile or brittle nature of a material is the Pugh ratio (B/G) (Pugh and "XCII. 1954). According to Pugh, the threshold value for "B/G" ratio is 1.75. A material which possess a value of Pugh ratio greater than 1.75 is considered to be more ductile and if the value exist below this range, the material will be brittle. Herein for the selected $AGeF_3$ (A = Ga and In) compounds, the computed Pugh ratio is observed to be 4.31 for $InGeF_3$ and 4.31 for $GaGeF_3$ which confirm the ductile nature of both the materials, as can be seen in the Table 2. The property of a metal to be easily cut (machined) allows for the removal of the material with a good finish at a reasonable price. Good machinability materials (free machining materials) can be cut rapidly, readily achieve a good finish, and do not put a lot of stress on the tooling. The "μ_M" is the parameter of machinability index which describes the cutting ability of a material and is measured employing the expression as;

$$\mu_M = \frac{B}{C_{44}} \tag{7}$$

The computed values of "μ_M" for both the ternary $AGeF_3$ (A = Ga and In) halides Perovskites are displayed in Table 2. The machinability index for $InGeF_3$ is 2.87 and that for $GaGeF_3$ is 2.99, which shows that such materials are appropriate for use in industrial applications due to improved greasing characters and reduced frictions. In the field of mechanics, hardness is a crucial quantity that expresses how resistant a material is to corrosion. Depending on the bulk and shear moduli, the following expression can be used to determine a material's Vickers hardness.

$$H_v = 2\left(\frac{G^3}{B^2}\right)^{0.585} - 3 \tag{8}$$

The values of "H_v" computed for both the fluoroperovskites compounds are displayed in Table 2, and the results predict that $InGeF_3$ is little harder than $GaGeF_3$. Based on these precise reported results of mechanical properties for $AGeF_3$ (A = Ga and In) compounds, we deem its application in many modern sustainable electronic gadgets. Based on these precise reported results of mechanical properties for $AGeF_3$ (A = Ga and In) compounds, we deem its application in many modern sustainable electronic gadgets.

3.4 The analysis of an optical properties

To observe and predict the fundamental plus derived optical response of germanium based fluoroperovskites $AGeF_3$ (A = Ga and In) compounds, the TB-mBJ

exchange–correlation potential is employed and the description of estimated parameters are reported in upcoming headlines.

3.4.1 The complex dielectric function

The complex dielectric constant $\varepsilon(\omega)$ delivers foundation for computation of all the basic optical reactions and can be expressed as:

$$\varepsilon(\omega) = \varepsilon_1(\omega) + i\varepsilon_2(\omega) \tag{9}$$

In the above Eq. (9), the $\varepsilon(\omega)$ is the complex function, $\varepsilon_1(\omega)$ shows the real part of $\varepsilon(\omega)$ and $\varepsilon_2(\omega)$ represents the imaginary component of dielectric function. The real "$\varepsilon_1(\omega)$" component of the complex "$\varepsilon(\omega)$" dielectric function is described by the famous Kramers–Kronig relation (Gorges et al. 1995).

$$\varepsilon_1(\omega) = 1 + \frac{2}{\pi} P \int_0^{\omega} \frac{\omega' \varepsilon_2(\omega') d\omega'}{\omega'^2 - \omega'^2} \tag{10}$$

The expression above defines $\varepsilon_1(\omega)$ which shows the electric polarizability and absorptive actions of the materials. The real component of "$\varepsilon(\omega)$" for both $AGeF_3$ (A = Ga and In) compounds is depicted in Fig. 5a while the Fig. 5b represents the "$\varepsilon_2(\omega)$" (imaginary part) within the incident photon energy of 0–40 eV. The static real part "$\varepsilon_1(0)$" of the dielectric function at 0 eV incident photon energy is same for both the materials and is observed to be 4.5. The spectrum of both the compounds for increases exponentially from the zero frequency limit and reaches to a maximum value of 7.88 and 7.72 for $GaGeF_3$ and $InGeF_3$ respectively. Figure 5 also depict an imaginary component "$\varepsilon_2(\omega)$" for both the $GaGeF_3$ and $InGeF_3$ compounds and it is very obvious from the Fig. 5 that the threshold values for both the selected materials occurs at the origin. Both compounds have a large peak at about 6–8 eV incident photon energies caused by the transitions from CB states to occupied VB states. These peaks play a critical role in the overall internal response of $AGeF_3$ (A = Ga and In) and are caused by the 5*p*-states of A (A = Ga and In).

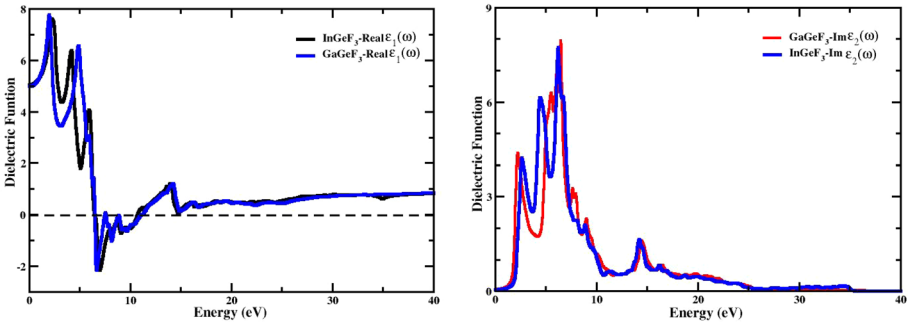

Fig. 5 The real "$\varepsilon_1(\omega)$" and imaginary "$\varepsilon_2(\omega)$" component of complex dielectric function of $AGeF_3$ (A = Ga and In) compounds

3.4.2 The optical conductivity

The following relation can be used to define the phenomena of electronic conductivity caused by electromagnetic radiation in terms of optical conductivity:

$$\delta(\omega) = \frac{2w_{cv}\hbar\omega}{E_0^2} \tag{11}$$

The optical conductivity plot, described in Fig. 6, can be used to analyze the conduction phenomena. It shows that the phenomenon of optical conduction starts at about 0.98 eV energy level and reaches its greatest position of 6382 Ohm^{-1} cm^{-1} at about 6 eV for $GaGeF_3$ and 6487 Ohm^{-1} cm^{-1} followed by a sharp drop in oscillations. The graph of optical conductivity shows that the selected compounds possess high optical response at low incident photon energy levels.

3.4.3 The absorption coefficient

This part computes the plot of the absorption coefficient. The following relationships can be used to compute the absorption coefficient $I(\omega)$.

$$I(\omega) = \frac{4\pi\kappa\omega}{\lambda} \tag{12}$$

The Fig. 7 depict an absorption coefficient of both the materials within the incident photon energies of 0 eV up to 40 eV and the analysis shows that the absorption starts at 0.98 eV. The conductivity plot behavior and the trend of band gaps are both in good agreement with the threshold point value. The strong absorption spectrum maxima is observed at about 6–8 eV, and is found to be 135 cm^{-1} for $GaGeF_3$ and 128 cm^{-1} for $InGeF_3$. The absorption coefficient decreases as the incident photon energy increases and reaches to zero at nearly 36 eV. This shows that both the materials are sensitive to the incident light at low energy ranges. Therefore, it is evident from absorption spectra that these compounds have a broad capacity for absorption in the nearly ultra-violet region, particularly at 7 eV.

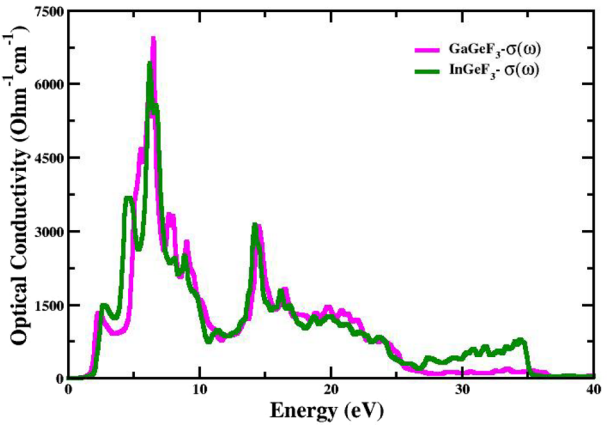

Fig. 6 The optical conductivity "$\delta(\omega)$" for indium based $AGeF_3$ (A = Ga and In) fluoroperovskites compounds

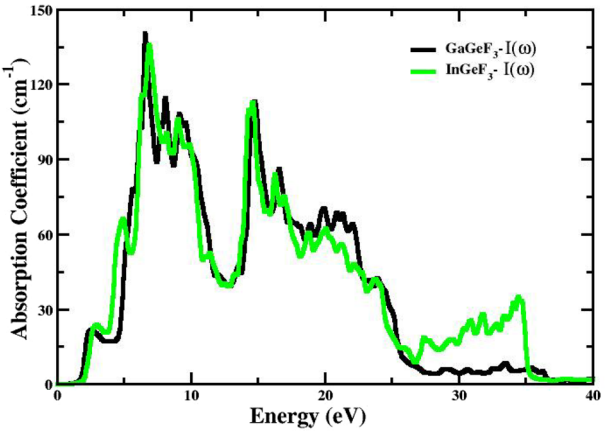

Fig. 7 The absorption coefficient "$I(\omega)$" for indium based $AGeF_3$ (A = Ga and In) fluoroperovskites compounds

3.4.4 The refractive index and extinction coefficient

The refractive index "$\eta(\omega)$" and extinction coefficient "$\kappa(\omega)$" for indium based $AGeF_3$ (A = Ga and In) fluoroperovskites compounds are investigated and analyzed here within the incident photon energies range of 0–40 eV. One of the primary properties that distinguishes an optical materials is its refractive index. The "$\eta(\omega)$" (refractive index) determines how much light is twisted or refracted when it crosses the boundary between two media. When building multi-element systems, optical designers must comprehend the refractive indices of each element in order to precisely specify how light will behave across the whole optical pathway. Optical designers select materials based on their capacity to bend light. The maximum refractive index for both the materials occurs at low 3–4 eV incident photon energies. The refractive index knowledge is essential for many optoelectronic devices, including solar cells, photonic crystals, and detectors. The computed value of extinction coefficient "$\kappa(\omega)$" is the proportion of a light beam's maximum to minimum transmission as it travels through an optical train using polarization. The spectrum of "$\kappa(\omega)$" is depicted in Fig. 8. It is concluded that the major peak of "$\kappa(\omega)$" for both the compounds are observed at the energy range of 6–8 eV.

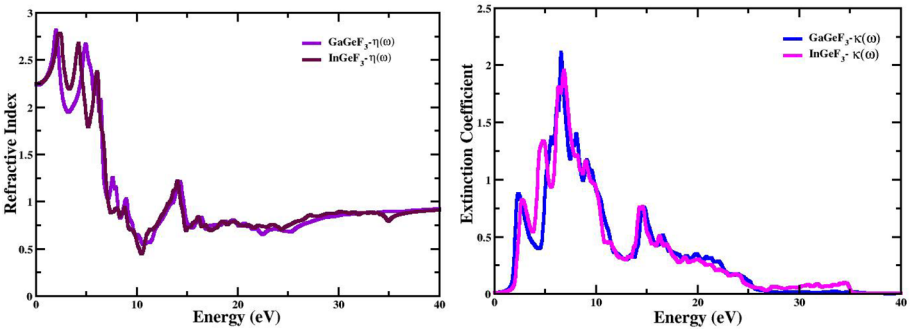

Fig. 8 The refractive index "$\eta(\omega)$" and extinction coefficient "$\kappa(\omega)$" for indium based $AGeF_3$ (A = Ga and In) fluoroperovskites compounds

3.4.5 The energy loss function

The energy-loss function, which establishes the likelihood of an inelastic scattering event, the energy-loss distribution, and the scattering angular distribution, is intimately related to the electron inelastic interaction with a material. The energy-loss function shows how a solid reacts to an external electromagnetic disturbance. Figure 9 represent the energy loss function from 0 eV up to 40 eV and it is concluded that the dominant response to an electromagnetic disturbance for both the materials occurs at the incident photon of low energy ranges. In summary, the germanium based $AGeF_3$ (A = Ga and In) fluoroperovskites compounds possesses high absorption coefficient, optical conductivity, refractive index and energy loss function at the low incident photon energies, which ensures that the selected materials can be applicable in many modern optoelectronic industries for various devices.

4 Conclusions

The comprehensive investigations of structural, optoelectronic, and mechanical properties of germanium based $AGeF_3$ (A = Ga and In) halides Perovskites is done using DFT computational approach within the framework of WIEN2K. Based on the reported computation of these properties, it is concluded that:

- The germanium based $AGeF_3$ (A = Ga and In) halides Perovskites possess in cubic crystalline structure. The tolerance factor and other structural properties indicates the structural stability and formation of both the materials.
- In electronic properties it is concluded that these compounds are narrow and an indirect band gap semiconductors from (R-M) with a band gap of 1.48 eV for $InGeF_3$ and 0.98 eV for $GaGeF_3$.
- The $AGeF_3$ (A = Ga and In) halides Perovskites are found to be mechanically stable, anisotropic, ductile and hard to scratch.
- The investigations of optical properties shows that both the materials hold high absorption coefficient, optical conductivity, refractive index and energy loss function at the

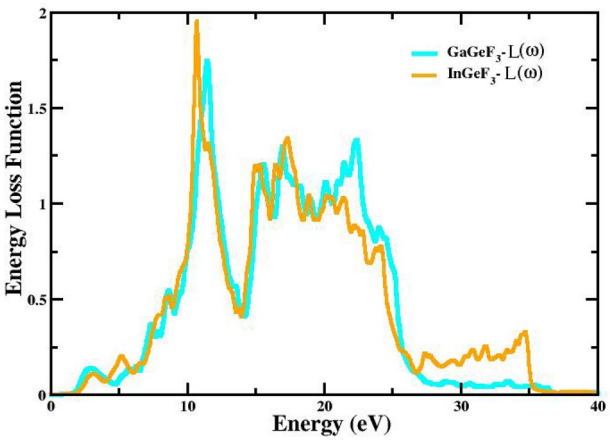

Fig. 9 The energy loss function "$L(\omega)$" for indium based $AGeF_3$ (A = Ga and In) fluoroperovskites compounds

low incident photon energies, which ensures the sensitivity of $AGeF_3$ (A = Ga and In) halides Perovskites up to the band gap energies.

Acknowledgements The authors extend their appreciation to the Deanship of Scientific Research at King Khalid University Abha 61421, Asir, Kingdom of Saudi Arabia for funding this work through the Small Groups Project under grant number RGP.1/123/43. The authors also would like to thank Princess Nourah bint Abdulrahman University Researchers Supporting Project number (PNURSP2023R9), Princess Nourah bint Abdulrahman University, Riyadh, Saudi Arabia for supporting this project.

Author contributions All authors contributed equally in the article in conceptualization, investigation, analysis, writing original draft, review and editing.

Declarations

Conflict of interest The authors declare no competing interests.

References

Ahmed, T., et al.: Physical properties of rare earth perovskites $CeMO_3$ (M= Co, Cu) in the context of density functional theory. Mater. Today Commun. **29**, 102973 (2021)

Alam, M.S., Saiduzzaman, M., Biswas, A., Ahmed, T., Sultana, A., Hossain, K.M.: Tuning band gap and enhancing optical functions of $AGeF_3$ (A= K, Rb) under pressure for improved optoelectronic applications. Sci. Rep. **12**(1), 8663 (2022)

Avram, C.N., Brik, M.G., Tanaka, I., Avram, N.M.: Electron–phonon interaction in the V^{2+}: $CsCaF_3$ laser crystal: geometry of the [VF6] 4−complex in the 4T2g excited state. Phys. B Condens. Matter **355**(1–4), 164–171 (2005)

Bartel, C.J., et al.: New tolerance factor to predict the stability of perovskite oxides and halides. Sci. Adv. **5**(2), eaav0693 (2019)

Berastegui, P., Hull, S., Eriksson, S.G.: A low-temperature structural phase transition in $CsPbF_3$. J. Phys. Condens. Matter **13**(22), 5077 (2001)

Blaha, P., Schwarz, K., Sorantin, P., Trickey, S.B.: Full-potential, linearized augmented plane wave programs for crystalline systems. Comput. Phys. Commun. **59**(2), 399–415 (1990)

Blaha, P., Schwarz, K., Madsen, G. K. H., Kvasnicka, D., Luitz, J.: "wien2k," An Augment. Pl. wave+ local orbitals Progr. Calc. Cryst. Prop. **60** (2001)

Bloomstein, T.M., Liberman, V., Rothschild, M., Hardy, D.E., Goodman, R.B.: Optical materials and coatings at 157 nm. Emerg Lithogr Technol III **3676**, 342–349 (1999)

Camargo-Martínez, J.A., Baquero, R.: Performance of the modified Becke–Johnson potential for semiconductors. Phys. Rev. B **86**(19), 195106 (2012)

Charifi, Z., Baaziz, H., Hassan, F.E.H., Bouarissa, N.: High pressure study of structural and electronic properties of calcium chalcogenides. J. Phys. Condens. Matter **17**(26), 4083 (2005)

Chen, D., Li, Y., Li, X., Hong, X., Fan, X., Savidge, T.: Key difference between transition state stabilization and ground state destabilization: increasing atomic charge densities before or during enzyme–substrate binding. Chem. Sci. **13**(27), 8193–8202 (2022)

Chi, E.O., Kim, W.S., Hur, N.H.: Nearly zero temperature coefficient of resistivity in antiperovskite compound $CuNMn_3$. Solid State Commun. **120**(7–8), 307–310 (2001)

Daniels, R.R., Margaritondo, G., Heaton, R.A., Lin, C.C.: Experimental study of the electronic structure of $KMgF_3$. Phys. Rev. B **27**(6), 3878 (1983)

de Lucas, M.C.M., Rodriguez, F., Moreno, M.: Excitation and emission thermal shifts in ABF3: Mn^{2+} perovskites: coupling with impurity vibrational modes. J. Phys. Condens. Matter **7**(38), 7535 (1995)

Donaldson, J., Williams, G. V. M., Raymond, S. G.: Characterization of a fluoroperovskite based fibre coupled optical dosimeter for radiotherapy (2014)

Dufek, P., Blaha, P., Schwarz, K.: Applications of Engel and Vosko's generalized gradient approximation in solids. Phys. Rev. B **50**(11), 7279 (1994)

El haj Hassan, F., Akbarzadeh, H., Hashemifar, S.J., Mokhtari, A.: Structural and electronic properties of matlockite MFX (MSr, Ba, Pb; XCl, Br, I) compounds. J. Phys. Chem. Solids **65**(11), 1871–1878 (2004)

Erum, N., Iqbal, M.A.: Mechanical and magneto-opto-electronic investigation of transition metal based fluoro-perovskites: an ab-initio DFT study. Solid State Commun. **264**, 39–48 (2017)
Fan, X., et al.: Reversible switching of interlayer exchange coupling through atomically thin VO_2 via electronic state modulation. Matter **2**(6), 1582–1593 (2020)
Frantsevich, I. N.: Elastic constants and elastic moduli of metals and insulators. *Ref. B.* (1982)
Gorges, E., Grosse, P., Theiss, W.: The Kramers–Kronig-relation of effective dielectric functions. Z. Für Phys. B Condens. Matter **97**(1), 49–54 (1995)
Hansson, T., Oostenbrink, C., van Gunsteren, W.: Molecular dynamics simulations. Curr. Opin. Struct. Biol. **12**(2), 190–196 (2002)
Haq, M.A., Saiduzzaman, M., Asif, T.I., Shuvo, I.K., Hossain, K.M.: Ultra-violet to visible band gap engineering of cubic halide $KCaCl_3$ perovskite under pressure for optoelectronic applications: insights from DFT. RSC Adv. **11**(58), 36367–36378 (2021)
Hill, R.: The elastic behaviour of a crystalline aggregate. Proc. Phys. Soc. Sect. A **65**(5), 349 (1952)
Hossain, K.M.: First-principles calculations to investigate switching from semiconducting to metallic with enhanced mechanical and optoelectronic properties of $CsPbCl_3$ under pressure. Int. J. Mater. Res. **113**(9), 833–846 (2022)
Jamal, M., Bilal, M., Ahmad, I., Jalali-Asadabadi, S.: IRelast package. J. Alloys Compd. **735**, 569–579 (2018)
Jong, U.-G., Yu, C.-J., Kye, Y.-H., Choe, Y.-G., Hao, W., Li, S.: First-principles study on structural, electronic, and optical properties of inorganic Ge-based halide perovskites. Inorg. Chem. **58**(7), 4134–4140 (2019)
Khondoker, S., Saiduzzaman, M., Hossain, K. M., Sajal, W. R., Rahman, M. A.: First-principles calculations to investigate the physical properties of silicate perovskites $ASiO_3$ (A= Al, In) using density functional theory. Indian J. Phys. 1–11 (2022)
Kim, W.S., Chi, E.O., Kim, J.C., Choi, H.S., Hur, N.H.: Close correlation among lattice, spin, and charge in the manganese-based antiperovskite material. Solid State Commun. **119**(8–9), 507–510 (2001)
Körbel, S., Marques, M.A.L., Botti, S.: Stability and electronic properties of new inorganic perovskites from high-throughput ab initio calculations. J. Mater. Chem. C **4**(15), 3157–3167 (2016)
LABRIM, H.: Electronic, optical and thermoelectric properties of the $CsMF_3$ (M= Si or Ge) fluoro-perovskites
Lahoz, F., Villacampa, B., Alcala, R.: The tetragonal to orthorhombic structural phase transition in $RbCaF_3$ single crystals: influence on the local environment of different nickel probes. J. Phys. Chem. Solids **58**(6), 881–892 (1997)
Li, G., et al.: Near-infrared responsive Z-scheme heterojunction with strong stability and ultra-high quantum efficiency constructed by lanthanide-doped glass. Appl. Catal. B Environ. **311**, 121363 (2022)
Liu, X., Liu, J., Yang, H., Huang, B., Zeng, G.: Design of a high-performance graphene/SiO_2–Ag periodic grating/MoS_2 surface plasmon resonance sensor. Appl. Opt. **61**(23), 6752–6760 (2022)
Manaa, H., Guyot, Y., Moncorge, R.: Spectroscopic and tunable laser properties of Co^{2+}-doped single crystals. Phys. Rev. B **48**(6), 3633 (1993)
Mitro, S.K., Saiduzzaman, M., Asif, T.I., Hossain, K.M.: Band gap engineering to stimulate the optoelectronic performance of lead-free halide perovskites $RbGeX_3$ (X= Cl, Br) under pressure. J. Mater. Sci. Mater. Electron. **33**(17), 13860–13875 (2022a)
Mitro, S.K., Saiduzzaman, M., Biswas, A., Sultana, A., Hossain, K.M.: Electronic phase transition and enhanced optoelectronic performance of lead-free halide perovskites $AGeI_3$ (A= Rb, K) under pressure. Mater. Today Commun. **31**, 103532 (2022b)
Molla, M.R., Saiduzzaman, M., Asif, T.I., Dujana, W.A., Hossain, K.M.: Electronic phase transition from semiconducting to metallic in cubic halide $CsYbCl_3$ perovskite under hydrostatic pressure. Phys. B Condens. Matter **630**, 413650 (2022)
Mooney, C. Z.: Monte carlo simulation, no. 116. Sage (1997)
Nishimatsu, T., et al.: Band structures of perovskite-like fluorides for vacuum-ultraviolet-transparent lens materials. Jpn. J. Appl. Phys. **41**(4A), L365 (2002)
Obot, I.B., Macdonald, D.D., Gasem, Z.M.: Density functional theory (DFT) as a powerful tool for designing new organic corrosion inhibitors. Part 1: an overview. Corros. Sci. **99**, 1–30 (2015)
Pugh, S.F.: XCII. Relations between the elastic moduli and the plastic properties of polycrystalline pure metals. Lond. Edinb. Dublin Philos. Mag. J. Sci. **45**(367), 823–843 (1954)
Santello, M., Toni, N., Volterra, A.: Astrocyte function from information processing to cognition and cognitive impairment. Nat. Neurosci. **22**(2), 154–166 (2019)
Seddik, T., Khenata, R., Merabiha, O., Bouhemadou, A., Bin-Omran, S., Rached, D.: Elastic, electronic and thermodynamic properties of fluoro-perovskite $KZnF_3$ via first-principles calculations. Appl. Phys. A **106**(3), 645–653 (2012)

Shuvo, I.K., Saiduzzaman, M., Asif, T.I., Haq, M.A., Hossain, K.M.: Band gap shifting of halide perovskite $CsCaBr_3$ from ultra-violet to visible region under pressure for photovoltaic applications. Mater. Sci. Eng. B **278**, 115645 (2022)

Sohail, M., et al.: First-principal investigations of electronic, structural, elastic and optical properties of the fluoroperovskite $TlLF_3$ (L= Ca, Cd) compounds for optoelectronic applications. RSC Adv. **12**(12), 7002–7008 (2022)

Vaitheeswaran, G., et al.: High-pressure structural study of fluoro-perovskite $CsCdF_3$ up to 60 GPa: a combined experimental and theoretical study. Phys. Rev. B **81**(7), 75105 (2010)

Voigt, W.: Lehrbuch der Kristallphysik (Textbook of crystal physics). *BG Teubner, Leipzig und Berlin* (1928)

Wang, J., Yip, S., Phillpot, S.R., Wolf, D.: Crystal instabilities at finite strain. Phys. Rev. Lett. **71**(25), 4182 (1993)

Wang, S., Wang, B., He, S., Wang, Y., Cheng, J., Li, Y.: Enhancing the photovoltaic performance of planar heterojunction perovskite solar cells via introducing binary-mixed organic electron transport layers. New J. Chem. **47**(10), 5048–5055 (2023)

Wei, Y., et al.: High-performance visible to near-infrared broadband Bi_2O_2Se nanoribbon photodetectors. Adv. Opt. Mater. **10**(23), 2201396 (2022)

Wu, X.-Y., Wang, K., Wang, H., Lu, B., Gao, Y.-P., Wang, C.: The nonlinear effects and applications of gain doped whispering-gallery mode cavities. Europhys. Lett. (2022)

Zhang, Z., et al.: Effects of solder thickness on interface behavior and nanoindentation characteristics in Cu/Sn/Cu microbumps. Weld. World **66**(5), 973–983 (2022)

Zheng, C., et al.: Hybrid offline programming method for robotic welding systems. Robot. Comput. Integr. Manuf. **73**, 102238 (2022)

Zhong, C., Li, H., Zhou, Y., Lv, Y., Chen, J., Li, Y.: Virtual synchronous generator of PV generation without energy storage for frequency support in autonomous microgrid. Int. J. Electr. Power Energy Syst. **134**, 107343 (2022a)

Zhong, Q., Chen, Y., Zhu, B., Liao, S., Shi, K.: A temperature field reconstruction method based on acoustic thermometry. Measurement **200**, 111642 (2022b)

Authors and Affiliations

Mudasser Husain[1] · Nasir Rahman[1] · Mongi Amami[2] · Tahir Zaman[3] · Mohammad Sohail[1] · Rajwali Khan[1] · Abid Ali Khan[4] · Saima Ahmad Shah[5] · Saeedullah[6] · Aurangzeb Khan[7,8] · Ali H. Reshak[9,10,11] · Nora Hamad Al-Shaalan[12] · Sarah Alharthi[13,14] · Saif A. Alharthy[15,16] · Mohammed A. Amin[13] · Vineet Tirth[17,18]

Mudasser Husain
mudasserhusain01@gmail.com

1 Department of Physics, University of Lakki Marwat, Lakki Marwat 28420, KPK, Pakistan

2 Department of Chemistry, College of Sciences Abha, King Khalid University, Abha, Saudi Arabia

3 Department of Mathematics, Govt Post Graduate College, Karak, KPK, Pakistan

4 Department of Chemical Sciences, University of Lakki Marwat, Lakki Marwat 28420, KPK, Pakistan

5 Department of Physics, Shaheed Benazir Bhutto Women University, Peshawar, Pakistan

6 Institute of Physics, Gomal University, Dera Ismail Khan 29220, KP, Pakistan

[7] Department of Physics, Abdul Wali Khan University, Mardan 23200, KPK, Pakistan

[8] University of Lakki Marwat, Lakki Marwat 28420, KPK, Pakistan

[9] Physics Department, College of Science, University of Basrah, Basrah, Iraq

[10] Department of Instrumentation and Control Engineering, Faculty of Mechanical Engineering, CTU in Prague, Technicka 4, 166 07 Prague 6, Czech Republic

[11] Center of Excellence Geopolymer and Green Technology, (CEGeoGTech), University Malaysia Perlis, 01007 Kangar, Perlis, Malaysia

[12] Department of Chemistry, College of Science, Princess Nourah bint Abdulrahman University, P.O. Box 84428, Riyadh 11671, Saudi Arabia

[13] Department of Chemistry, College of Science, Taif University, P.O. Box 11099, Taif 21944, Saudi Arabia

[14] Center of Advanced Research in Science and Technology, Taif University, P.O. Box 11099, Taif 21944, Saudi Arabia

[15] Department of Medical Laboratory Sciences, Faculty of Applied Medical Sciences, King Abdulaziz University, P.O. Box 80216, Jidda 21589, Saudi Arabia

[16] King Fahd Medical Research Center, King Abdulaziz University, P.O. Box 80216, Jidda 21589, Saudi Arabia

[17] Mechanical Engineering Department, College of Engineering, King Khalid University, 61421 Abha, Asir, Kingdom of Saudi Arabia

[18] Research Center for Advanced Materials Science (RCAMS), King Khalid University, Guraiger, P.O. Box 9004, 61413 Abha, Asir, Kingdom of Saudi Arabia